Available online at www.sciencedirect.com
SCIENCE DIRECT®
Chemical Physics 304 (2004) 103–120
Chemical Physics
www.elsevier.com/locate/chemphys

The phase space CCS approach to quantum and semiclassical molecular dynamics for high-dimensional systems

Dmitrii V. Shalashilin *, Mark S. Child

Physical and Theoretical Chemistry Laboratory, Oxford University, South Parks Road, Oxford OX1 3QZ, UK

Received 11 January 2003; accepted 3 June 2004
Available online 27 July 2004

Abstract

The paper reviews the new coupled coherent states (CCS) technique for solution of the time-dependent Schrödinger equation in phase space, as a method for simulating the quantum dynamics of high-dimensional systems. The method is fully quantum although it exploits grids of CS guided by classical mechanics. As distinct from other trajectory guided approaches, the trajectories that carry the coherent states are governed by the classical equivalent of a quantum mechanically ordered Hamiltonian, that ensures optimal cancellation in quantum mechanical coupling terms. The resulting smoothness in the kernel of the integro-differential equation is therefore well adapted for Monte Carlo sampling. The simplest non-unitary version of the theory also obviates the need to invert large overlap matrices. Unitary corrections are also included and the analytical connection with uncoupled semiclassical initial value representation (IVR) techniques is described in detail. A variety of applications are presented.

1. Introduction

The semiclassical limit of quantum mechanics, which has received considerable attention in the last few decades, is naturally in phase space. The method of choice, particularly for high-dimensional systems, is to employ an initial value representation (IVR) [1], based on the propagation of a swarm of phase adapted classical trajectories sampled from suitably chosen initial coordinates and momenta. Various reviews are available in the literature [2–7]. The earliest, so-called frozen Gaussian (FG) approach, due to Heller [8], has been superseded more recently by the Herman–Kluk (HK) method [3,9,10] in which an additional prefactor, dependent on the monodromy matrix of the trajectory in question, is included for each member of the swarm, in order to ensure that the coherent state propagator reduces, in the stationary phase limit, to the correct semiclassical Van Vleck form [11] in coordinate or momentum representation [12]. Monte Carlo sampling of the swarm leads to excellent scaling properties with respect to dimensionality, while retaining quantum interference effects, and a large number of applications have been reported [13–22]. Additional references may be found in the reviews cited above.

Schemes for the phase space formulation of exact quantum mechanics have also been attempted, starting first with the suggestion [23,24] that the wavefunction may be expanded in a basis of trajectory guided gausian functions. A variety of applications of this general approach have been given [25–31]. In addition the present authors [32–36] have outlined a more systematic development of the theory, by exploiting special properties of the harmonic oscillator coherent states, in a manner analogous to second quantization. One important aspect is that the coherent states form a continuous basis, which casts the time-dependent Schrödinger equation into an exact integro-differential form for the coherent state amplitudes, in which the Hamiltonian appears as a kernel rather than a matrix. Secondly, the kernel may be reduced to a small smooth function, by working in a trajectory guided basis, with the trajectories moving not under the bare classical Hamiltonian, but under the coherent state average of the suitably ordered quantum operator, $H_{\mathrm{ord}}(q,p) = \langle q,p|\hat{H}_{\mathrm{ord}}|q,p\rangle$. Further details are given below.

* Corresponding author. Fax: +44-1865-275410.
E-mail address: dmitrii@katja.chem.umass.edu (D.V. Shalashilin).

0301-0104/$ - see front matter © 2004 Elsevier B.V. All rights reserved.
doi:10.1016/j.chemphys.2004.06.013

One valuable outcome of this integro-differential formulation is to provide insight into the logical basis of the semiclassical IVR propagation methods. For example Heller's FG method [8], which was formulated on heuristic grounds, is found to correspond to complete neglect of the quantum mechanical kernel, while the HK method, which was previously derived [3,9,10,12,37] as a Gaussian smoothening of Van Vleck semiclassical propagator in coordinate space, was recently shown to be consistent with locally quadratic coupling by the kernel, around the trajectory of interest [35,38]. Secondly, replacement of the integral by a discrete sum yields a computational scheme, termed the coupled coherent states (CCS) method, which is analogous to those of Metiu and co-workers [23,24], Martinez et al. [25–29] and Burghardt et al. [30,31], except that steps have been taken to minimize the magnitude of the quantum mechanical coupling. Consequently, the integro-differential form provides a natural root for the development of both semiclassical and quantum mechanical phase space theories of molecular dynamics. The various connections are represented pictorially in Fig. 1.

An attractive feature of our CCS quantum initial value representations is that smoothness of the integro-differential kernel allows Monte Carlo sampling of the trajectory swarm, for which the number of grid points, N, ideally scales quadratically with the number of degrees of freedom, M

$$N \propto M^2. \tag{1}$$

This is in sharp contrast with the usual exponential growth of the number of basis functions

$$N = l^M, \tag{2}$$

where l is the number of grid points per degree of freedom. This scaling property is normally only exploited in quantum mechanical applications involving ground states [39] because Monte Carlo quadrature is unsuited to the more oscillatory integrands arising from excited states. The essence of our CCS technique, is to use classical mechanics to eliminate the dominant quantum oscillations, and thereby to allow computations for high-dimensional systems.

The purposes of this paper are to outline the interconnections between different strands of the IVR phase space approach to the molecular dynamics of high-dimensional systems and to outline the achievements of the CCS method. Section 2 is devoted to notation and properties of coherent states, while the following three sections lay out details of the exact quantum mechanical equations. Section 3 deals with the simplest case in which the phase space basis is fixed for all time. Extensions to handle evolution of the wavefunction in a trajectory guided basis are described in Section 4. Section 5 then gives analogous equations for the exact quantum mechanical propagator. Section 6 of the main text concerns the relationship between the exact quantum mechanics set out in Sections 4 and 5 and the semiclassical IVR approaches with FG and Herman–Kluk (HK) propagators. Discretization to the exact CCS equations, as employed for practical computations, with good scaling properties, on high-dimensional systems are discussed in Section 6, where comparisons are also made with other approaches involving trajectory guided coherent states. A point of particular interest

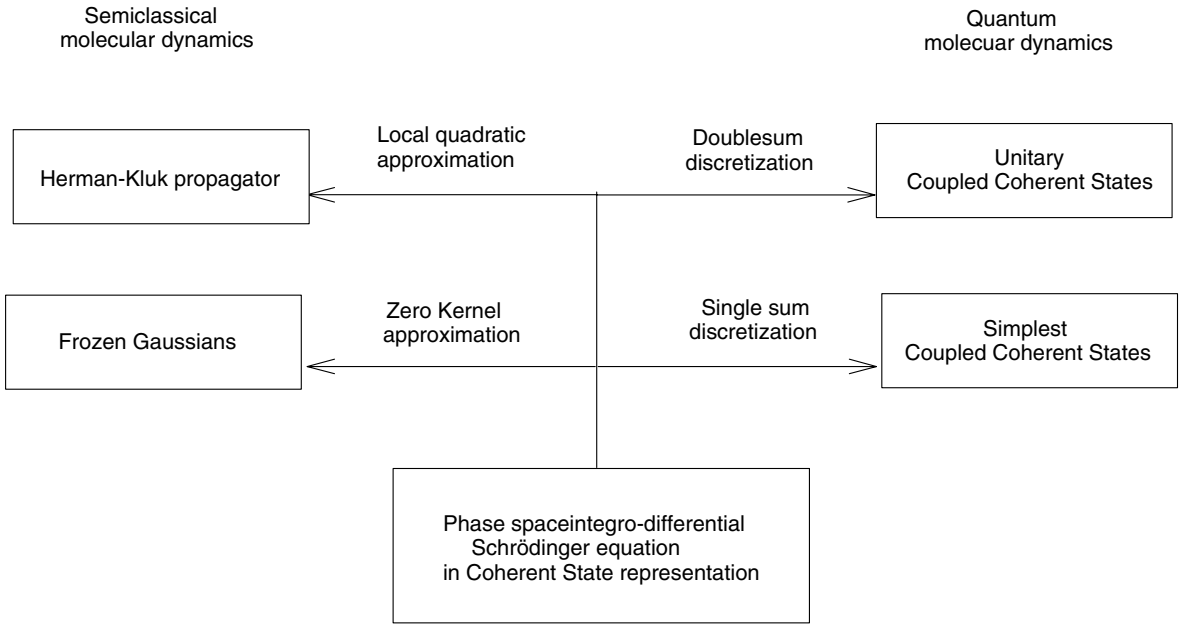

Fig. 1. Integro-differential phase space form of Schrödinger equations as a root to various semiclassical and quantum methods of propagation on random trajectory guided grids.

relates to the treatment of non-orthogonality in the coherent state basis. The article concludes in Section 8, with a discussion of the strengths and weaknesses of quantum propagation on trajectory guided grids of CS.

Although our main interest is multidimensional quantum mechanics, for simplicity all formulas in the main body of the article are given for 1D case. The corresponding generic multidimensional formulas are presented in Appendix A.

2. Coherent state properties and notations

First, we briefly summarize relevant properties of the coherent states (CS), using so-called $|z\rangle$ notation from the physics literature [40–42], rather than the $|q,p\rangle$ notation commonly employed by chemical physicists [2–7]. The difference lies in a phase factor, $\exp\left(\frac{ipq}{2\hbar}\right)$ because

$$\langle x|z\rangle = \left(\frac{\gamma}{\pi}\right)^{\frac{1}{4}} \exp\left(-\frac{\gamma}{2}(x-q)^2 + \frac{\mathrm{i}}{\hbar}p(x-q) + \frac{\mathrm{i}pq}{2\hbar}\right), \tag{3}$$

while

$$\langle x|p,q\rangle = \left(\frac{\gamma}{\pi}\right)^{\frac{1}{4}} \exp\left(-\frac{\gamma}{2}(x-q)^2 + \frac{\mathrm{i}}{\hbar}p(x-q)\right), \tag{4}$$

in which γ is an arbitrary coordinate width parameter. Both are seen to be eigenfunctions of the scaled creation and annihilation operators

$$\begin{aligned} \hat{a} &= \left(\frac{\gamma}{2}\right)^{\frac{1}{2}}\hat{q} + \frac{\mathrm{i}}{\hbar}\left(\frac{1}{2\gamma}\right)^{\frac{1}{2}}\hat{p}, \\ \hat{a}^\dagger &= \left(\frac{\gamma}{2}\right)^{\frac{1}{2}}\hat{q} - \frac{\mathrm{i}}{\hbar}\left(\frac{1}{2\gamma}\right)^{\frac{1}{2}}\hat{p}. \end{aligned} \tag{5}$$

Thus

$$\hat{a}|z\rangle = z|z\rangle \quad \langle z|\hat{a}^\dagger = \langle z|z^*, \tag{6}$$

where

$$\begin{aligned} z &= \left(\frac{\gamma}{2}\right)^{\frac{1}{2}}q + \frac{\mathrm{i}}{\hbar}\left(\frac{1}{2\gamma}\right)^{\frac{1}{2}}p, \\ z^* &= \left(\frac{\gamma}{2}\right)^{\frac{1}{2}}q - \frac{\mathrm{i}}{\hbar}\left(\frac{1}{2\gamma}\right)^{\frac{1}{2}}p. \end{aligned} \tag{7}$$

As an important consequence it proves convenient to express a generic Hamiltonian in the ordered form

$$\widehat{H}(\hat{p},\hat{q}) = \widehat{H}(\hat{a},\hat{a}^\dagger) = \widehat{H}_{\mathrm{ord}}(\hat{a}^\dagger,\hat{a}), \tag{8}$$

such that the powers of $\hat{a}^\dagger$ precede those of $\hat{a}$. It then follows from Eq. (6) that a typical matrix element reduces to

$$\langle z_2|\widehat{H}|z_1\rangle = \langle z_2|z_1\rangle H_{\mathrm{ord}}(z_2^*, z_1), \tag{9}$$

in which $H_{\mathrm{ord}}(z_2^*, z_1)$ is the classical analogue of $\widehat{H}_{\mathrm{ord}}(\hat{a}^\dagger,\hat{a})$ with $\hat{a}^\dagger$ and $\hat{a}$ replaced by z_2^* and z_1, respectively.

The next step is to notice that Eq. (7) allows the use of (z,z^*) as a pair of canonical classical variables in place of (q,p) and it is convenient, for later smoothing of the CCS integro-differential equation kernel, to define a system of trajectories moving under the diagonal part of $H_{\mathrm{ord}}(z^*,z)$ according to Hamilton's equations in the transformed variables.

$$\frac{\mathrm{d}z}{\mathrm{d}t} = -\frac{\mathrm{i}}{\hbar}\frac{\partial H_{\mathrm{ord}}(z^*,z)}{\partial z^*}, \quad \frac{\mathrm{d}z^*}{\mathrm{d}t} = \frac{\mathrm{i}}{\hbar}\frac{\partial H_{\mathrm{ord}}(z^*,z)}{\partial z}. \tag{10}$$

Planck's constant enters into these purely classical equations simply because it is involved into the definition of new canonical pair (7). One can of course revert to the normal (p,q) equations, with the help of Eq. (7), but the resulting Hamiltonian $H_{\mathrm{ord}}(p,q) = H_{\mathrm{cl}} + H_{\mathrm{com}}$ will differ from the normal classical form by terms arising from the commutator between powers of $\hat{a}$ and $\hat{a}^\dagger$, which will be discussed in Section 6.2 in more details.

It might seem at first sight that the definition of CS (5) and (7), which also clearly applies with $|z\rangle$ replaced by $|q,p\rangle$, violates the uncertainty principle, except that $\hat{a}$ and $\hat{a}^\dagger$ are non-hermitian and hence non-observable. It is readily verified in fact that any coherent state with real γ has the minimum allowed uncertainty product

$$\Delta p \Delta q = \frac{\hbar}{2}. \tag{11}$$

Another centrally important property is the overcompleteness of the coherent states, as expressed by the identity [40]

$$|z\rangle = \frac{1}{\pi}\int \mathrm{d}^2z' |z'\rangle\langle z'|z\rangle, \quad \mathrm{d}^2z = \frac{\mathrm{d}q\,\mathrm{d}p}{2\hbar}, \tag{12}$$

which may be seen as a consequence of the uncertainty principle, in the sense that any coherent state may be expressed as a superposition of all others, including itself, with the overlap integral given by

$$\langle z'|z\rangle = \exp\left(z'^*z - \frac{|z'|^2}{2} - \frac{|z|^2}{2}\right). \tag{13}$$

Looked at in another way, Eq. (12) may be viewed as a consequence of the identity operator

$$\widehat{I} = \frac{1}{\pi}\int \mathrm{d}^2z |z\rangle\langle z|, \tag{14}$$

from which one may express any ket $|\Psi\rangle$ in terms of its coherent state representation $\langle z|\Psi\rangle = \Psi(z)$ in the form

$$|\Psi\rangle = \widehat{I}|\Psi\rangle = \frac{1}{\pi}\int \mathrm{d}^2z |z\rangle\langle z|\Psi\rangle = \frac{1}{\pi}\int \mathrm{d}^2z |z\rangle\Psi(z), \tag{15}$$

entirely analogous (apart from the factor $1/\pi$) to the corresponding form in the usual coordinate representation $\Psi(x) = \langle x|\Psi\rangle$

$$|\Psi\rangle = \widehat{I}|\Psi\rangle = \int \mathrm{d}x\,|x\rangle\langle x|\Psi\rangle = \int \mathrm{d}x\,|x\rangle\,\Psi(x). \tag{16}$$

To take a simple example, the well-known harmonic oscillator state expansion [40]

$$|z\rangle = \mathrm{e}^{-|z|^2/2}\sum_{n=0}^{\infty}\frac{1}{\sqrt{n!}}z^n|\psi_n\rangle, \tag{17}$$

implies that

$$\langle z|\psi_n\rangle = \frac{(z^*)^n}{\sqrt{n!}}\exp\left[-\frac{1}{2}|z|^2\right]. \tag{18}$$

The theory that follows is based on similar coherent state representations for more complicated systems.

As a final note, let us look again at the relation between the above z-notations for coherent states, which is favored by physicists [40], to the (p,q) notation often used by theoretical chemists [2–7]. As mentioned above, the only difference is an extra phase term in the coherent state expression, $|z\rangle = |p,q\rangle\exp\left(\frac{\mathrm{i}pq}{2\hbar}\right)$, which is compensated by a slightly unusual form for the classical action

$$S_z = \int\left[\frac{\mathrm{i}\hbar}{2}\left(z^*\frac{\mathrm{d}z}{\mathrm{d}t} - \frac{\mathrm{d}z^*}{\mathrm{d}t}z\right) - H_{\mathrm{ord}}(z^*,z)\right]\mathrm{d}t, \tag{19}$$

$$= \int\left[\frac{1}{2}\left(p\frac{\mathrm{d}q}{\mathrm{d}t} - q\frac{\mathrm{d}p}{\mathrm{d}t}\right) - H_{\mathrm{ord}}(p,q)\right]\mathrm{d}t \tag{20}$$

in place of the traditional form

$$S_{p,q} = \int\left[p\frac{\mathrm{d}q}{\mathrm{d}t} - H_{\mathrm{ord}}(p,q)\right]\mathrm{d}t. \tag{21}$$

Integrating by parts one can easily show that

$$\int_0^t\frac{1}{2}\left(p\frac{\mathrm{d}q}{\mathrm{d}t} - q\frac{\mathrm{d}p}{\mathrm{d}t}\right)\mathrm{d}t + \frac{\mathrm{i}p(t)q(t)}{2\hbar} - \frac{\mathrm{i}p(0)q(0)}{2\hbar} = \int_0^t p\frac{\mathrm{d}q}{\mathrm{d}t}\mathrm{d}t, \tag{22}$$

where $p(0)q(0)$ and $p(t)q(t)$ are initial and final points of a trajectory, so that

$$|z(t)\rangle\exp\left(\frac{\mathrm{i}S_z}{\hbar}\right)\langle z(0)| = |p(t)q(t)\rangle\exp\left(\frac{\mathrm{i}S_{pq}}{\hbar}\right)\langle p(0)q(0)|, \tag{23}$$

and of course the two notations are identical. The argument in favor of the z-notation is, as we will see later, that it leads to a more compact form for many of the equations.

3. Phase space quantum dynamics in a static basis

The time-dependent Schrödinger equation

$$\frac{\mathrm{d}|\Psi\rangle}{\mathrm{d}t} = -\frac{\mathrm{i}}{\hbar}\widehat{H}|\Psi\rangle, \tag{24}$$

may be cast into the coherent state integro-differential form

$$\frac{\mathrm{d}\langle z|\Psi\rangle}{\mathrm{d}t} = -\frac{\mathrm{i}}{\hbar}\int\langle z|\widehat{H}|z'\rangle\langle z'|\Psi\rangle\frac{\mathrm{d}^2z'}{\pi} = -\frac{\mathrm{i}}{\hbar}\int\langle z|z'\rangle H_{\mathrm{ord}}(z^*,z')\langle z'|\Psi\rangle\frac{\mathrm{d}^2z'}{\pi}, \tag{25}$$

by inserting the identity in Eq. (14) between $\widehat{H}$ and $|\Psi\rangle$, closing the result with the bra $\langle z|$ and using Eq. (9) to evaluate the matrix element.

The integral in Eq. (25), which is taken over a static grid $|z'\rangle$, must normally be approximated in practical applications by the finite sum in Eq. (26)

$$\frac{\mathrm{d}\langle z_i|\Psi\rangle}{\mathrm{d}t} \simeq -\frac{\mathrm{i}}{\hbar}\sum_j\langle z_i|\widehat{H}|z_j\rangle\langle z_j|\Psi\rangle\frac{\Delta^2 z_j}{\pi}, \tag{26}$$

which implies an equivalent approximation

$$\widehat{I} = \frac{1}{\pi}\int\mathrm{d}^2z\,|z\rangle\langle z| \simeq \sum_j|z_j\rangle\langle z_j|\frac{\Delta^2 z_j}{\pi}, \tag{27}$$

for the identity operator, where Δz_j is the appropriate grid spacing. Previously the discretization (27) was used for propagation on regular static phase space grid with the help short time semiclassical HK propagator [43,44]. The validity of Eq. (27), on a regular grid, clearly depends on the accuracy of trapezoidal quadrature for Gaussian integrals, or by the sensitivity of the value of the sum to the chosen origin of the grid. Burant and Baptista [44] recommend maximum spacings $\Delta q \leqslant (2\sqrt{\gamma})^{-1}$ and $\Delta p = \hbar\sqrt{\gamma}$, in order to obtain double precision accuracy. The resulting maximum phase space cell size, $\hbar/2$ per coherent state, is somewhat smaller than the area h, suggested by von Neumann [45], who was the first to address this question.

A similar discussion was given by the present authors [32], in the context of a model study of Morse oscillator dynamics propagated by Eq. (26) on a finite static grid, using parameters previously employed to test hybrid mechanics [46–48] and short time coherent state propagation [43]. Results of acceptable accuracy, shown in Fig. 2 after propagation for roughly four time periods, were obtained with a cell size, $\Delta q\Delta p = 1.4\hbar$, somewhat larger than that suggested in [44], provided that the chosen 15×11 grid, was large enough to avoid edge effects. Results obtained by random Monte Carlo sampling on a static grid were, however, much less satisfactory.

A disadvantage of the discretization (26) is that the norm $\langle\Psi|\Psi\rangle$ is not automatically conserved, though the extent of norm conservation can be used as a measure of the accuracy of the propagation. Unitarity is, however, preserved by employing an alternative discrete representation for the identity

$$\widehat{I} = \sum_{j,k}|z_j\rangle\left(\mathbf{\Omega}^{-1}\right)_{jk}\langle z_k|, \tag{28}$$

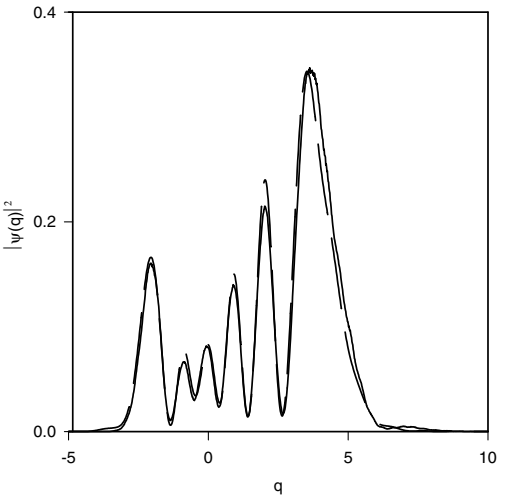

Fig. 2. Wave function propagated in Morse potential for four periods on a rectangular static grid of CS (dashed line) compared with split operator result (solid line).

in a non-orthogonal coherent state basis, with overlap matrix elements $\mathbf{\Omega}_{ij} = \langle z_i | z_j \rangle$. We use $\mathbf{\Omega}$ rather than the more usual $\mathbf{S}$ for the overlap matrix to avoid later confusion with the classical action. The corresponding propagation equation becomes

$$\frac{\mathrm{d}\langle z_i|\Psi\rangle}{\mathrm{d}t} = -\frac{\mathrm{i}}{\hbar}\sum_{j,k}\langle z_i|\widehat{H}|z_j\rangle\left(\mathbf{\Omega}^{-1}\right)_{jk}\langle z_j|\Psi\rangle. \tag{29}$$

The first application of the propagation on a phase space grid with discretization (28) is the famous hybrid mechanics method suggested by Huber and Heller [46–48]. Their approach, which relied on thawed Gaussian short time propagator rather then coupled Eq. (29), was later improved by introducing an efficient iterative scheme for inverting the overlap matrix [49].

Eq. (29) typically gives more accurate results than Eq. (26), for a given grid size, but at computational cost, in inverting the overlap matrix. Both methods are fast and efficient for low-dimensional problems, but both are limited to rectangular grids, possibly moving as a whole, under some 'guiding path' [32,43,44], because the oscillatory character of $\langle z|\Psi\rangle$ precludes the use of Monte Carlo sampling methods. Consequently, the computational effort scales exponentially with the dimensionality of the system. The following section shows how semiclassical modifications can facilitate random sampling techniques, by smoothing the terms on the right-hand sides of Eqs. (26) and (29).

4. Trajectory guided coupled coherent states

Crucial improvements are achieved by allowing the CS centers $[p(t), q(t)]$ to move along classical trajectories, determined by Eq. (10). Inclusion of the additional term arising from the time dependence of the basis, transforms Eq. (25) to

$$\begin{aligned}\frac{\mathrm{d}\langle z|\Psi\rangle}{\mathrm{d}t} &= \langle \dot{z}|\Psi\rangle + \langle z|\dot{\Psi}\rangle \\ &= \int\left[\langle \dot{z}|z'\rangle - \frac{\mathrm{i}}{\hbar}\langle z|\widehat{H}|z'\rangle\right]\langle z'|\Psi\rangle\frac{\mathrm{d}^2 z'}{\pi},\end{aligned} \tag{30}$$

where, by virtue of the time derivative of (13)

$$\langle \dot{z}|z'\rangle = \langle z|z'\rangle\left\{\frac{\mathrm{d}z^*}{\mathrm{d}t}z' - \frac{1}{2}\left[z\frac{\mathrm{d}z^*}{\mathrm{d}t} + \frac{\mathrm{d}z}{\mathrm{d}t}z^*\right]\right\}. \tag{31}$$

It follows from Eqs. (10) and (31) that Eq. (30) can be written as

$$\frac{\mathrm{d}\langle z|\Psi\rangle}{\mathrm{d}t} = \int\langle z|z'\rangle\left\{\frac{\mathrm{i}}{\hbar}\frac{\mathrm{d}S_z}{\mathrm{d}t} - \frac{\mathrm{i}}{\hbar}\delta^2 H_{\mathrm{ord}}\left(z^*, z'\right)\right\}\langle z'|\Psi\rangle\frac{\mathrm{d}^2 z'}{\pi}, \tag{32}$$

where S_z is the classical action (19) along the trajectory defined by the diagonal ($z' = z$) part of ordered Hamiltonian $H_{\mathrm{ord}}(\mathbf{z}^*, \mathbf{z})$ and

$$\begin{aligned}\delta^2 H_{\mathrm{ord}}\left(z^*, z'\right) &= H_{\mathrm{ord}}\left(z^*, z'\right) - H_{\mathrm{ord}}(z^*, z) \\ &\quad - \frac{\partial H_{\mathrm{ord}}(z^*, z)}{\partial z}\left(z' - z\right).\end{aligned} \tag{33}$$

Note also that

$$\int\langle z|z'\rangle\langle z'|\Psi\rangle\frac{\mathrm{d}^2 z'}{\pi} = \langle z|\Psi\rangle, \tag{34}$$

so that

$$\begin{aligned}\frac{\mathrm{d}\langle z|\Psi\rangle}{\mathrm{d}t} &= \frac{\mathrm{i}}{\hbar}\frac{\mathrm{d}S_z}{\mathrm{d}t}\langle z|\Psi\rangle - \frac{\mathrm{i}}{\hbar} \\ &\quad \times\int\langle z|z'\rangle\,\delta^2 H_{\mathrm{ord}}\left(z^*, z'\right)\langle z'|\Psi\rangle\frac{\mathrm{d}^2 z'}{\pi^M}.\end{aligned} \tag{35}$$

Consequently, by expressing the amplitudes in the form

$$\langle z|\Psi\rangle = C(z(t))\exp\left(\frac{\mathrm{i}}{\hbar}S_z\right), \tag{36}$$

the coefficients $C(z(t))$ are given by

$$\begin{aligned}\frac{\mathrm{d}C(z(t))}{\mathrm{d}t} &= -\frac{\mathrm{i}}{\hbar}\int\langle z|z'\rangle\delta^2 H_{\mathrm{ord}}\left(z^*, z'\right)C\left(z'(t)\right) \\ &\quad \times\exp\left(\frac{\mathrm{i}}{\hbar}\left(S_{z'} - S_z\right)\right)\frac{\mathrm{d}^2 z'}{\pi},\end{aligned} \tag{37}$$

which is the working equation of the CCS method.

Eq. (37) has several attractive features, compared with Eq. (25). First, the factorization in Eq. (36) means that $C(z(t))$ is smoother in both z' and t than $\langle z|\Psi\rangle$. Second, the presence of the action difference, coupled with the smoothness of $C(\mathbf{z}(t))$ allows Monte Carlo evaluation of the integral on the right-hand side. Thirdly the expansion of $\delta^2 H_{\mathrm{ord}}(z^*, z')$ begins with the second-order term

$$\delta^2 H_{\mathrm{ord}}\left(z^*, z'\right) = \frac{1}{2}\frac{\partial^2 H_{\mathrm{ord}}}{\partial z^2}\left(z' - z\right)^2 + \cdots, \tag{38}$$

which means that $\delta^2 H_{\rm ord}(z^*,z')$ vanishes for $z'=z$ and small for close lying CS. Moreover the overlap $\langle z|z'\rangle$ vanishes for remote CS. Thus, the coupling is almost always small and sparse. Finally, Liouwille theorem ensures that $\mathrm{d}^2z'(t)=\mathrm{d}^2z'(0)$ which means that the integration in Eq. (37) can be performed over CS initial conditions. Overall Eq. (37) may be seen as a quantum mechanical initial value representation, well adapted to solution by Monte Carlo sampling methods.

5. The trajectory guided quantum propagator

As a means to investigate the quantum mechanical status of the semiclassical Herman–Kluk method [3,9,10], Miller [38] applied the arguments of the previous section to a propagation equation of the form

$$|\Psi\rangle = \mathrm{e}^{-\mathrm{i}Ht/\hbar}|\Psi_0\rangle = \int |z'(t)\rangle R(z',t)\,\mathrm{e}^{\mathrm{i}S/\hbar}\langle z'(0)|\Psi(0)\rangle\frac{\mathrm{d}^2z'}{\pi}, \tag{39}$$

except that Miller's trajectories were assumed to run under the classical Hamiltonian, rather than the reordered Hamiltonian of Eq. (8). To maintain contact with the previous section, we express the equivalent of Eq. (39) in the form

$$|\Psi\rangle = \int |z'(t)\rangle D(z',t)\exp\left(\frac{\mathrm{i}}{\hbar}S_{z'}\right)\frac{\mathrm{d}^2z'}{\pi}, \tag{40}$$

where

$$D(z',t) = R(z',t)\langle z'(0)|\Psi(0)\rangle. \tag{41}$$

Substituting this into Schrödinger equation and closing it with $\langle z|$ we have

$$\int\left\{\langle z|z'\rangle\left(\frac{\mathrm{d}D(z',t)}{\mathrm{d}t}+\frac{\mathrm{i}}{\hbar}\frac{\mathrm{d}S_{z'}}{\mathrm{d}t}D(z',t)\right)+\left\langle z|\dot{z'}\right\rangle D(z',t)\right\}\mathrm{e}^{\mathrm{i}S_{z'}/\hbar}\frac{\mathrm{d}^2z'}{\pi} = -\frac{\mathrm{i}}{\hbar}\int\langle z|\widehat{H}|z'(t)\rangle D(z',t)\exp\left(\frac{\mathrm{i}}{\hbar}S_{z'}\right)\frac{\mathrm{d}^2z'}{\pi}. \tag{42}$$

It follows, by combining the explicit expression

$$\langle z|\dot{z'}\rangle = \langle z|z'(t)\rangle\left\{z^*\frac{\mathrm{d}z'}{\mathrm{d}t}-\frac{1}{2}\left[z'\frac{\mathrm{d}z'^*}{\mathrm{d}t}+\frac{\mathrm{d}z'}{\mathrm{d}t}z'^*\right]\right\}, \tag{43}$$

with Hamilton's Eq. (10) that

$$\int\langle z|z'\rangle\frac{\mathrm{d}D(z',t)}{\mathrm{d}t}\exp\left(\frac{\mathrm{i}}{\hbar}(S_{z'}-S_z)\right)\frac{\mathrm{d}^2z'}{\pi} = -\frac{\mathrm{i}}{\hbar}\int\langle z|z'\rangle\delta^2H'^*_{\rm ord}(z^*,z')D(z',t)\times\exp\left(\frac{\mathrm{i}}{\hbar}(S_{z'}-S_z)\right)\frac{\mathrm{d}^2z'}{\pi}, \tag{44}$$

where

$$\delta^2H'^*_{\rm ord}(z^*,z') = H_{\rm ord}(z^*,z') - H_{\rm ord}(z'^*,z') - \frac{\partial H_{\rm ord}(z'^*,z')}{\partial z'^*}(z^*-z'^*), \tag{45}$$

which differs slightly from $\delta^2H_{\rm ord}(z^*,z')$ in Eq. (33). A factor $\exp\left(-\frac{\mathrm{i}}{\hbar}S_z\right)$ has been inserted in either side of Eq. (44), in order to smooth the integrand. Equations equivalent to (44) in (p,q) notation were obtained by Miller [38].

The connection between C and D determined by Eqs. (37) and (44), respectively, may be obtained by comparing Eqs. (36) and (39) in the form

$$\langle z|\Psi\rangle = C(z,t)\exp\left(\frac{\mathrm{i}}{\hbar}S_z\right) = \int\langle z|z'\rangle D(z',t)\exp\left(\frac{\mathrm{i}}{\hbar}S_{z'}\right)\frac{\mathrm{d}^2z'}{\pi}. \tag{46}$$

Notice also, by virtue of Eqs. (34) and (36), that

$$C(z,t)\exp\left(\frac{\mathrm{i}}{\hbar}S_z\right) = \int\langle z|z'\rangle C(z',t)\exp\left(\frac{\mathrm{i}}{\hbar}S_{z'}\right)\frac{\mathrm{d}^2z'}{\pi}, \tag{47}$$

though Eqs. (46) and (47) do not imply an identity between C and D because different integral representations of $\langle z|\Psi\rangle = C(z,t)\exp\left(\frac{\mathrm{i}}{\hbar}S_z\right)$ are possible.

6. Analytical connections with Heller and Herman–Kluk theories

6.1. Heller frozen Gaussian theory

Since the kernel of integro-differential equation Eq. (37) is always small, the simplest (zero kernel approximation) solution is obtained by completely neglecting the right-hand side, so that $C(z,t)$ is time independent. The resulting wavefunction

$$|\Psi(t)\rangle = \int|z(t)\rangle C(z,0)\exp\left(\frac{\mathrm{i}}{\hbar}S_z\right)\frac{\mathrm{d}^2z}{\pi}, \tag{48}$$

takes the form employed in Heller's frozen Gaussians method, in which the time dependence of the wave function comes only from classical motion of CS and classical action term $\exp\left(\frac{\mathrm{i}}{\hbar}S_z\right)$. An improvement to FG comes from the fact that quantum corrections are included in the Hamiltonian that drives the trajectories, and in the action term S_z. As a result, zero point energy effects are taken into account. Thus, our CCS integro-differential equation provides a rigorous derivation of the FG method, which was originally suggested by elegant heuristic arguments [8].

6.2. Herman–Kluk theory

Derivation of the Herman–Kluk propagator is more difficult. It was first given by Miller [38], by solving the propagator equation (44) for the coefficient D, in a locally quadratic approximation to the classical Hamiltonian. Later the present authors [35] gave an equivalent solution to the CCS equation (37) for the coefficient C, now in a locally quadratic approximation to the ordered Hamiltonian of Eq. (8). It is most convenient for present purposes to follow Miller's derivation of the propagator coefficient D, and then to evaluate the integral in Eq. (46) for the wavefunction coefficient C.

For exact correspondence with Miller it is convenient to assume that propagating wave function is itself a coherent state (i.e. $|\Psi(0)\rangle = |z_i\rangle$) and to use Eq. (41) to replace $D(z',t)$ by $R(z',t)\langle z'(0)|z_i\rangle$, so that (44) goes over to

$$\int \langle z|z'(t)\rangle \frac{\mathrm{d}R(z',t)}{\mathrm{d}t} \exp\left(\frac{\mathrm{i}}{\hbar}(S_{z'} - S_z)\right) \times \langle z'(0)|z_i\rangle \frac{\mathrm{d}^2 z'}{\pi} = -\frac{\mathrm{i}}{\hbar}\int \langle z|z'(t)\rangle \delta^2 H'^{*}_{\mathrm{ord}}(z^*, z') R(z',t) \times \exp\left(\frac{\mathrm{i}}{\hbar}(S_{z'} - S_z)\right)\langle z'(0)|z_i\rangle \frac{\mathrm{d}^2 z'}{\pi}. \tag{49}$$

The next step is to assume a locally quadratic approximation to the classical potential, about a reference trajectory $q(t)$

$$V[q(t) + \Delta q] = V[q(t)] + V'[q(t)]\Delta q + \frac{V''[q(t)]\Delta q^2}{2}, \tag{50}$$

in which case the reordered Hamiltonian differs from classical Hamiltonian simply by a local zero point energy term

$$H_{\mathrm{ord}}(z^*, z) = H_{\mathrm{cl}}(z^*, z) + \left(\frac{\hbar^2\gamma}{4m} + \frac{V''}{4\gamma}\right). \tag{51}$$

Similarly for the action

$$S_z = S_z^{\mathrm{cl}} - \left(\frac{\hbar^2\gamma}{4m} + \frac{V''}{4\gamma}\right)t. \tag{52}$$

A second consequence of the local quadratic approximation is that the coupling terms $\delta^2 H_{zz}$ and $\delta^2 H'^{*}_{\mathrm{ord}}$ truncate at the second order terms

$$\delta^2 H_{\mathrm{ord}}(z^*, z') = \frac{1}{2}\frac{\partial^2 H_{\mathrm{cl}}}{\partial z^2}(z' - z)^2, \tag{53}$$

$$\delta^2 H'^{*}_{\mathrm{ord}}(z^*, z') = \frac{1}{2}\frac{\partial^2 H_{\mathrm{cl}}}{\partial z'^{*2}}(z^* - z'^{*})^2, \tag{54}$$

where the second derivatives of the Hamiltonian are given by

$$\frac{\partial^2 H_{\mathrm{cl}}}{\partial z^2} = \frac{\partial^2 H_{\mathrm{cl}}}{\partial z'^{*2}} = \left(-\frac{\hbar^2\gamma}{4m} + \frac{V''}{4\gamma}\right), \qquad \frac{\partial^2 H_{\mathrm{cl}}}{\partial z \partial z^*} = 2\left(\frac{\hbar^2\gamma}{4m} + \frac{V''}{4\gamma}\right). \tag{55}$$

A third consequence is that the dynamics may be linearized around the reference trajectory $z(t)$, in the sense that the displacement $\Delta z(t)$ of a neighboring trajectory starting at $z(0) + \Delta z(0)$ evolves under the monodromy matrix $M(t)$ as

$$\begin{pmatrix} \Delta z(t) \\ \Delta z^*(t) \end{pmatrix} = \begin{pmatrix} M_{zz}(t) & M_{zz^*}(t) \\ M_{z^*z}(t) & M_{z^*z^*}(t) \end{pmatrix} \begin{pmatrix} \Delta z(0) \\ \Delta z^*(0) \end{pmatrix}. \tag{56}$$

The time dependence of $\mathbf{M}$, which is later dropped for notational compactness, is determined by Hamilton's Eq. (10) for z and z^*

$$\begin{pmatrix} \dot{M}_{zz} & \dot{M}_{zz^*} \\ \dot{M}_{z^*z} & \dot{M}_{z^*z^*} \end{pmatrix} = -\frac{\mathrm{i}}{\hbar}\begin{pmatrix} \frac{\partial^2 H_{\mathrm{cl}}}{\partial z^* \partial z} & \frac{\partial^2 H_{\mathrm{cl}}}{\partial z^{*2}} \\ -\frac{\partial^2 H_{\mathrm{cl}}}{\partial z^2} & -\frac{\partial^2 H_{\mathrm{cl}}}{\partial z \partial z^*} \end{pmatrix} \begin{pmatrix} M_{zz} & M_{zz^*} \\ M_{z^*z} & M_{z^*z^*} \end{pmatrix}. \tag{57}$$

Note also that the elements of M in the (z, z^*) notation are related to their (p, q) equivalents defined by the equation

$$\begin{pmatrix} \Delta p(t) \\ \Delta q(t) \end{pmatrix} = \begin{pmatrix} M_{pp}(t) & M_{pq}(t) \\ M_{qp}(t) & M_{qq}(t) \end{pmatrix} \begin{pmatrix} \Delta p(0) \\ \Delta q(0) \end{pmatrix}, \tag{58}$$

in the forms

$$\begin{aligned} M_{zz} &= \frac{1}{2}\left(M_{qq} + M_{pp} - i\gamma\hbar M_{qp} + \frac{\mathrm{i}}{\gamma\hbar}M_{pq}\right), \\ M_{zz^*} &= \frac{1}{2}\left(M_{qq} - M_{pp} + i\gamma\hbar M_{qp} + \frac{\mathrm{i}}{\gamma\hbar}M_{pq}\right), \\ M_{z^*z} &= \frac{1}{2}\left(M_{qq} - M_{pp} - i\gamma\hbar M_{qp} - \frac{\mathrm{i}}{\gamma\hbar}M_{pq}\right), \\ M_{z^*z^*} &= \frac{1}{2}\left(M_{qq} + M_{pp} + i\gamma\hbar M_{qp} - \frac{\mathrm{i}}{\gamma\hbar}M_{pq}\right). \end{aligned} \tag{59}$$

The final consequence of the locally quadratic approximation is that the solution $R(z',t)$ of Eq. (49) is independent of z', provided that z, z' and z_i are all driven by the same potential (50). Consequently, Eq. (49) may be rearranged to read

$$\frac{\mathrm{d}\ln R}{\mathrm{d}t} = -\frac{\mathrm{i}}{\hbar}\frac{1}{2}\frac{\partial^2 H_{zz}}{\partial z^2}\frac{I_2}{I_0}, \tag{60}$$

where

$$I_0 = \int \langle z|z'(t)\rangle \exp\left(\frac{\mathrm{i}}{\hbar}(S_{z'} - S_z)\right)\langle z'(0)|z_i(0)\rangle \frac{\mathrm{d}^2 z'}{\pi}, \tag{61}$$

and

$$I_2 = \int \langle z|z'(t)\rangle (z^* - z'^{*})^2 \times \exp\left(\frac{\mathrm{i}}{\hbar}(S_{z'} - S_z)\right)\langle z'(0)|z_i(0)\rangle \frac{\mathrm{d}^2 z'}{\pi}. \tag{62}$$

Miller [38] shows that

$$\frac{I_2}{I_0} = -2\frac{M_{z^*z}}{M_{zz}}. \tag{63}$$

We also demonstrate it in Appendix B of the present article. To conclude the argument it is convenient to define a phase modified Herman–Kluk coefficient

$$R_{\mathrm{HK}}(z,t) = R(z,t)\exp\left(-\frac{\mathrm{i}}{\hbar}\left(\frac{\hbar^2\gamma}{4m}+\frac{V''}{4\gamma}\right)t\right),$$

so that, with the help of Eq. (52)

$$R(z,t)\exp\left(\frac{\mathrm{i}}{\hbar}S_z\right) = R_{\mathrm{HK}}(z,t)\exp\left(\frac{\mathrm{i}}{\hbar}S_z^{\mathrm{cl}}\right). \tag{64}$$

One can now combine Eqs. (55), (60), (63) and (64), to read

$$\frac{\mathrm{d}\ln R_{\mathrm{HK}}}{\mathrm{d}t} = -\frac{\mathrm{i}}{2\hbar}\left[2\left(\frac{\hbar^2\gamma}{4m}+\frac{V''}{4\gamma}\right)-\left(-\frac{\hbar^2\gamma}{4m}+\frac{V''}{4\gamma}\right)\frac{M_{z^*z}}{M_{zz}}\right], \tag{65}$$

which, with the help of Eqs. (55) and (57), can be re-written as

$$\frac{\mathrm{d}\ln R_{\mathrm{HK}}}{\mathrm{d}t} = \frac{1}{2}\left[\frac{\dot{M}_{zz}}{M_{zz}}\right]. \tag{66}$$

Eventually, the solution of Eq. (66)

$$R_{\mathrm{HK}} = \sqrt{M_{zz}}, \tag{67}$$

yields the famous Herman–Kluk propagator formula

$$\begin{aligned}|\Psi(t)\rangle &= \mathrm{e}^{-\mathrm{i}\widehat{H}_{\mathrm{HK}}t/\hbar}|\Psi(0)\rangle \\ &= \int |z(t)\rangle\sqrt{M_{zz}}\exp\left(\frac{\mathrm{i}S_z^{\mathrm{cl}}}{\hbar}\right)\langle z(0)|\Psi(0)\rangle\frac{\mathrm{d}^2z}{\pi}.\end{aligned} \tag{68}$$

It is interesting to notice that the preexponential factor in Eq. (68) appears as a single element M_{zz} of the monodromy matrix, in the z-notation, a point which, to our knowledge, was only once previously recognized in the literature [50]. The compact form of (67) clearly demonstrates the advantage of the coherent state z-notation.

The application of similar arguments to the CCS equation (37), in a locally quadratic approximation to the ordered Hamiltonian yields two equivalent expressions for the matrix element of the HK propagator [35], according to whether the reference trajectory runs from z_i to $z_i(t)$ or from a variable point $z_f(0)$ to a fixed point z_f in time t. The most convenient form for practical purposes is

$$\begin{aligned}\langle z_f|\,\mathrm{e}^{-\mathrm{i}H_{\mathrm{HK}}t/\hbar}|z_i\rangle = \frac{\langle z_f|z_i(t)\rangle}{\sqrt{M_{z^*z^*}}}\exp\left\{\frac{1}{2}\delta z^*(M_{zz^*})(M_{z^*z^*})^{-1}\delta z^*\right. \\ \left.+\frac{\mathrm{i}}{\hbar}\left[S_{z_i}^{\mathrm{cl}}+\sigma_{z_i}\right]\right\},\end{aligned} \tag{69}$$

where $\delta z^* = z_f^* - z_i^*(t)$ and

$$\sigma = \frac{1}{2}\int_0^t\left(\partial^2 H_{\mathrm{ord}}/\partial z\partial z^* - H_{\mathrm{comm}}\right)\mathrm{d}t, \tag{70}$$

in which H_{comm} is the commutator term arising from the reordering. The same result may be derived either as a matrix element of a thawed Gaussian wavepacket [35,51], or by evaluating the integral in Eq. (47), with the coefficient D given by Eqs. (41) and (67). In the latter case the term σ vanishes, because the integrand in Eq. (70) vanishes in a local quadratic approximation to the classical Hamiltonian.

The strength of the results of this section lies in the demonstration that the Herman–Kluk prefactor may be attributed to the local quantum mechanical coupling between a coherent state $|z_i(t)\rangle$ and its immediate neighbors. As indicated by Miller [38] the method of derivation may also lead to future improvements in the form of the prefactor. It must be stressed, however, that a typical potential function is far from globally quadratic. Hence, any proper treatment of the dynamics requires an integral, or at least a sum, over contributions from many different trajectories.

It should also be noted that results equivalent to those Eq. (69) were derived by path integral method by Baranger et al. [52], again with locally quadratic approximation to the averaged classical Hamiltonian $H_{\mathrm{ord}}(z^*,z)$ and again reproducing a phase correction term equivalent to σ Eq. (70). The main result [52], which is a form for the thawed Gaussian wave function moving over the averaged Hamiltonian, is undoubtedly correct, but comments on its relevance to Herman–Kluk theory have raised some discussion [52–55]. Part of the controversy concerns the meaning of the term 'semi-classical', but there is also a significant computational point concerning the use of a single or multitrajectory thawed Gaussian wavepacket compared with a swarm of frozen wavepackets employed by Herman–Kluk method. To illustrate the difference test calculations have been performed in our group [56]. Our thawed wavepacket results for Morse oscillator, either in its classical or averaged form, yield highly accurate eigenvalues for the state closest in energy to that of the chosen trajectories, but the side band peaks are incorrectly separated from it by regular energy intervals determined by the frequency of chosen trajectory. On the other hand, a sufficiently large swarm of either frozen or thawed wavepackets changes the interference pattern in such a way that the power spectrum replaces the spurious side bands by peaks at the correct eigenvalues. This reinforces Heller's early contention that anharmonicity can only be properly included by using the overcompletness to decompose any central initial wavepacket into swarm of its immediate neighbors.

For systems with more then one degree of freedom we attempted to use thawed Gaussian in the multitrajectory context relying on the generic expression for the CS propagator

$$\mathrm{e}^{-\mathrm{i}\widehat{H}t/\hbar} = \int\int |z_f\rangle\langle z_f|\,\mathrm{e}^{-\mathrm{i}Ht/\hbar}|z_i\rangle\langle z_i|\frac{\mathrm{d}^2z_i}{\pi}\frac{\mathrm{d}^2z_f}{\pi}, \tag{71}$$

and using approximation (69) for the matrix elements, which is similar in spirit to a suggestion for extension of

Baranger's paper [52]. Our experience (although limited) shows that standard expression for HK propagator (68) seems to be more accurate because Eq. (69) relies on the additional approximation that all trajectories are driven by the quadratic Hamiltonian of the central reference trajectory z_i. Similar conclusion has been made recently in [57].

7. Discrete representations for the CCS equations

7.1. Non-unitary

Practical applications of the theory require that the integral in the CCS equation (37) or their propagator equivalent (42), should be replaced by a discrete sum. As discussed in Section 3, the discrete approximation to the identity, given by Eq. (27), is accurate to double precision provided that the regular grid spacing is less than the prescribed limits. The simplest discrete approximation is to employ a similar approximation when sampling from a Monte Carlo grid. Thus

$$\widehat{I} = \int |z(t)\rangle\langle z(t)| \frac{\mathrm{d}^2 z}{\pi} \simeq \widehat{I}_{\mathrm{CCS}} = \sum_{i=1,N} |z_i(t)\rangle\langle z_i(t)| \frac{\Delta^2 z_i}{\pi}, \tag{72}$$

where $\frac{\Delta^2 z_i}{\pi} = \frac{1}{(2\pi\hbar)}\Delta p_i \Delta q_i$ is the mean phase volume assigned to the ith CS. The CCS equation (37) then become

$$\frac{\mathrm{d}C_k}{\mathrm{d}t} = -\frac{\mathrm{i}}{\hbar}\sum_i \mathbf{\Omega}_{ki}\delta^2 H_{\mathrm{ord}}\left(z_k^*, z_i\right) C_i \exp\left(\frac{\mathrm{i}}{\hbar}(S_i - S_k)\right)\frac{\Delta^2 z_i}{\pi}. \tag{73}$$

which in matrix form reads

$$\dot{\mathbf{c}} = -\frac{\mathrm{i}}{\hbar}\mathbf{E}^*\delta^2\mathbf{H}\mathbf{\Delta}^2\mathbf{Z}\mathbf{E}\mathbf{c}, \tag{74}$$

where $\mathbf{\Omega}$ is overlap matrix, the elements of matrixes $\delta^2\mathbf{H}$ are given by

$$\delta^2\mathbf{H}_{ki} = \mathbf{\Omega}_{ki}\delta^2 H_{\mathrm{ord}}\left(z_k^*, z_i\right), \tag{75}$$

and $\mathbf{E}$ is a diagonal matrix with elements

$$\mathbf{E}_{ki} = \delta_{ki}\exp\left(\frac{\mathrm{i}}{\hbar}S_k\right). \tag{76}$$

The matrix $\mathbf{\Delta}^2\mathbf{Z}$, is also diagonal, with elements equal to the phase volume per coherent state

$$\mathbf{\Delta}^2\mathbf{Z}_{ki} = \delta_{ki}\frac{\Delta^2 z_i}{\pi}. \tag{77}$$

If importance sampling is used and N coherent states are distributed according to a distribution $f(z)$ then

$$\frac{\Delta^2 z_i}{\pi} = \frac{1}{N}\frac{1}{f(z_i)\pi}.$$

Due to the non-unitary nature of this discretization, the norm of the wavefunction is not preserved under Eq. (73). The computational effort for this scheme scales as the square of the number of trajectories.

7.2. Unitary

A computationally more expensive unitary representation that preserves the norm is obtained by employing the following exact representation for the identity in a finite non-orthogonal basis.

$$\widehat{I} = \int |z(t)\rangle\langle z(t)| \frac{\mathrm{d}^2 z}{\pi} \to \sum_{i,j} |z_i(t)\rangle(\mathbf{\Omega}^{-1})_{ij}\langle z_j(t)|, \tag{78}$$

where $(\mathbf{\Omega}^{-1})_{ij}$ is an element of the inverse overlap matrix with elements $\mathbf{\Omega}_{kl} = \langle \mathbf{z}_k | \mathbf{z}_l \rangle$. Two resulting unitary representations are given, one derived from the CCS equation (37) and the other from Miller's propagator variant (40). Starting with the CCS form, Eqs. (15) and (30) are replaced by

$$|\Psi\rangle = \sum_{ij} |z_i(t)\rangle(\mathbf{\Omega}^{-1})_{ij}\langle z_j(t)|\Psi\rangle = \sum_{ij} |z_i(t)\rangle(\mathbf{\Omega}^{-1})_{ij}\Psi_j \tag{79}$$

and

$$\frac{\mathrm{d}\Psi_k}{\mathrm{d}t} = \sum_{i,j}\left[\langle \dot{z}_k | z_i\rangle(\Omega^{-1})_{ij} - \frac{\mathrm{i}}{\hbar}\mathbf{\Omega}_{ki}H\left(z_k^*, z_i\right)(\Omega^{-1})_{ij}\right]\Psi_j. \tag{80}$$

The subsequent derivation, with $\Psi_i = C_i \exp\left(\frac{\mathrm{i}}{\hbar}S_i\right)$, proceeds similarly to that of Eq. (37), to yield the following analog of Eq. (73):

$$\frac{\mathrm{d}C_k}{\mathrm{d}t} = -\frac{\mathrm{i}}{\hbar}\sum_{i,j}\mathbf{\Omega}_{ki}\delta^2 H_{\mathrm{ord}}\left(z_k^*, z_i\right)(\Omega^{-1})_{ij}C_j \times \exp\left(\frac{\mathrm{i}}{\hbar}\left(S_j - S_k\right)\right). \tag{81}$$

Eq. (81) could also have been obtained directly from the discretization of Eq. (37) by replacing integral identity with the finite sum (78).

To obtain the discrete analog of Miller's form (44), we recognize that the integral representation for the wave function in Eq. (40) is a simple ansatz, rather than an outcome of the identity operation. Its discrete approximation is therefore

$$|\Psi\rangle \simeq \sum_{i,j}|z_i\rangle D_i \exp\left(\frac{\mathrm{i}}{\hbar}S_i\right), \tag{82}$$

so that, by comparison with (79), the coefficients D_i are related to the above C_j in the form

$$D_i \exp\left(\frac{\mathrm{i}}{\hbar}S_i\right) = \sum_j (\mathbf{\Omega}^{-1})_{ij}C_j \exp\left(\frac{\mathrm{i}}{\hbar}S_j\right). \tag{83}$$

Repetition of the argument in Section 5, starting from Eq. (82) yields

$$\sum_j \Omega_{ij} \exp\left(\frac{\mathrm{i}}{\hbar}(S_j - S_i)\right)\frac{\mathrm{d}D_j}{\mathrm{d}t} = -\frac{\mathrm{i}}{\hbar}\sum_j \Omega_{ij}\delta^2 H'^*_{\mathrm{ord}}(z_i^*, z_j)\exp\left(\frac{\mathrm{i}}{\hbar}(S_j - S_i)\right)D_j. \quad (84)$$

It follows, on multiplying through by $(\mathbf{\Omega}^{-1})_{ki}$, summing over i and rearranging that

$$\frac{\mathrm{d}D_k}{\mathrm{d}t} = -\frac{\mathrm{i}}{\hbar}\sum_{ij}(\Omega^{-1})_{ki}\mathbf{S}_{ij}\delta^2 H'^*_{\mathrm{ord}}(z_i^*, z_j)D_j \exp\left(\frac{\mathrm{i}}{\hbar}(S_j - S_k)\right). \quad (85)$$

In matrix form Eqs. (81) and (85) read as

$$\dot{\mathbf{c}} = -\frac{\mathrm{i}}{\hbar}\mathbf{E}^*\delta^2\mathbf{H}\mathbf{\Omega}^{-1}\mathbf{E}\mathbf{c} \quad (86)$$

and

$$\dot{\mathbf{d}} = -\frac{\mathrm{i}}{\hbar}\mathbf{E}^*\mathbf{\Omega}^{-1}\delta^2\mathbf{H}'^*\mathbf{E}\mathbf{d}, \quad (87)$$

where $\mathbf{\Omega}$ is the overlap matrix, the elements of matrix $\delta^2\mathbf{H}$ are given by (75) and those of $\delta^2\mathbf{H}'^*$ by

$$\delta^2\mathbf{H}'^*_{ki} = \mathbf{\Omega}_{ki}\delta^2 H'^*_{\mathrm{ord}}(z_k^*, z_i). \quad (88)$$

The difference between Eqs. (86) and (87) arises from the difference between the coefficients D_i and C_j in Eq. (83), the initial values of C_j being given by $\langle z_j(0)|\Psi(0)\rangle$, while those of D_i are the actual coefficients of $|z_i\rangle$ in Eq. (83). It may be verified by using manipulations similar to those in Section 4, that the following two expressions for the norm are preserved by Eqs. (86) and (87)

$$\langle\Psi|\Psi\rangle = \sum_{ij} C_i^*(\Omega^{-1})_{ij}\exp\left[\frac{\mathrm{i}}{\hbar}(S_j - S_i)\right]C_j = \sum_{ij} D_i^*\Omega_{ij}\exp\left[\frac{\mathrm{i}}{\hbar}(S_j - S_i)\right]D_j. \quad (89)$$

It is interesting to compare the above unitary forms with corresponding equations employed in the multiple spawned Gaussian (MSG) method of Martinez et al. [25–29]. Major differences are that the MSG technique involves the generation of new coherent states during the propagation (spawning) and that applications have made to non-adiabatic dynamics on several potential surfaces. The basic MSG equations are, however, identical in structure to Eq. (87) except for the composition of the coupling terms $\delta^2\mathbf{H}'^*$. The essential difference arises from the fact that the present classical trajectories are governed by the averaged Hamiltonian $H_{\mathrm{ord}}(z^*, z)$, which also determines the matrix elements in Eq. (32). Consequently, the action derivatives in the trajectory guided basis exactly cancel the diagonal matrix elements to produce traceless matrices $\delta^2\mathbf{H}$ and $\delta^2\mathbf{H}'^*$ in Eqs. (86) and (87). The equivalent matrices in MSG theory achieve only partial cancellation, because the trajectories and the classical action derivatives are determined by the classical, rather than the reordered Hamiltonian. The consequent reduction in the magnitude of the coupling terms means that the propagation can be converged with a larger time step.

Turning to the comparison between the non-unitary, single sum Eq. (74) and the unitary double sum forms Eqs. (86) and (87), the computational effort with both schemes is proportional to the square of the number of trajectories. For unitary Eqs. (86) and (87) the proportionality factor is greater than for the non-unitary propagation by Eq. (74), but the size of the trajectory sample is shown below to be smaller. Hence, the overall computational effort is roughly the same for both methods. The extent to which the norm is preserved under Eq. (74) provides a guide to the accuracy of the propagation, which is not available under Eqs. (86) and (87), because unitarity is guaranteed. The cancellation of diagonal terms becomes vital for the single sum non-unitary method, because our experience shows that a single sum discretization of Eq. (30) for the full CS amplitudes $\langle\mathbf{z}|\Psi\rangle$ seldom if ever converges, whereas Eqs. (73) and (74) for the smooth C coefficient yield meaningful results very quickly. The double sum equations work with partial cancellation and even Eq. (80), which includes large diagonal terms can be solved numerically with sufficiently small time step.

8. Applications and computational consideration

Various aspects of our previous applications [32–34,36] are used to illustrate the flexibility of the CCS method and to provide evidence on the scaling with dimensionality, convergence with respect to the number of trajectories and stability with respect to the propagation time.

8.1. Quantum mechanical tunneling

We first demonstrate the quantum mechanical correctness of the theory by obtaining tunneling splittings [33], for the model Hamiltonian

$$\widehat{H} = \frac{1}{2}\hat{p}^2 + k(x-a)^2(x+a)^2, \quad (90)$$

with $m = 2$, $k = 0.1$ and $a = 2$, which was previously used by Huber et al. [48] The first point of interest is that the diagonal elements of the reordered Hamiltonian, $H_{\mathrm{ord}}(z^*, z)$ imply an increase in the effective potential at the potential minima and a decrease at the maximum, as shown in Fig. 3. The magnitudes of these shifts depends on the coherent state parameter γ, which is optimally taken as $\gamma = m\omega_0/\hbar$, where ω_0 is the equilibrium vibrational frequency, in which case the positive shift at the minima closely approximates the zero-point energy. The

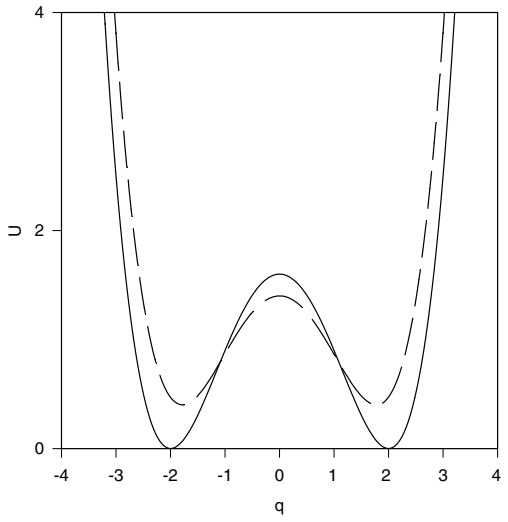

Fig. 3. Potential energy Eq. (90) and corresponding "reordered" potential.

downward shift of the maximum clearly facilitates the tunneling.

The main result is that the autocorrelation functions (ACFs)

$$\langle \Psi(0)|\Psi(t)\rangle = \left\langle \Psi(0)\left| \exp\left(-\frac{\mathrm{i}\widehat{H}t}{\hbar}\right)\right|\Psi(0)\right\rangle, \qquad (91)$$

illustrated in Fig. 4, show the characteristic beating pattern associated with tunneling between the two potential wells, whereas a comparable semiclassical HK calculation [62] yields only a regularly oscillatory ACF. The first four panels of Fig. 4 show results obtained by non-unitary single sum propagation Eq. (73), for various grid types and sizes, with the initial wavepacket $|\Psi(0)\rangle$ located in the right-hand potential well. Fig. 4(e) is the numerically exact ACF, obtained by split-operator propagation [59–61].

It is seen that the beat frequency is underestimated by the smallest (500 CS) Monte Carlo sample in Fig. 4(a), but well reproduced by all other CCS calculations. There is also evidence of irregularity in the ACF for the small (200 CS) Sobol quasirandom sample in Fig. 4(c), but results for the large (2000 CS) Monte Carlo and (500 CS) Sobol samples in Fig. 4(b) and (d) are almost quantitatively accurate up to the second zero in the ACF. However, the quality of the calculation progressively degrades at longer times, unless the size of the trajectory sample is increased. Nevertheless, the propagation time in Fig. 4 is sufficient to allow an accurate estimate of the tunneling eigenvalues The fast oscillations determine the mean of the tunneling eigenvalues and the splitting is given by $\Delta E = 2\pi\hbar/\Delta t$, where Δt is the time difference between the zeros of the ACF. More accurate estimates were obtained [33] by filter diagonalization [62–64] of the autocorrelation function.

A similar test calculation was also performed for a more challenging strongly non-separable two-dimensional model [66], with much deeper potential wells [33], for which as many as 10^4 randomly sampled trajectories were required to obtain a converged ACF, though only for times short compared with the beating period. Nevertheless, filter diagonalization of a 5×5 cross-correlation matrix allowed three-figure accurate estimates of the eight eigenvalues below the barrier. It should be added that HK propagation for the same model was equally well converged for a similar time period using 10^5 trajectories, selected by importance sampling, and that similar accuracy in the eigenvalues was obtained by filter diagonalization [62,65]. Given that computational effort for HK and CCS propagation scale linearly and quadratically, respectively, with the number of trajectories, the semiclassical HK scheme is the more efficient, on the basis of the above figures, although it should be recognized that the number of CCS trajectories could be significantly reduced by importance sampling.

8.2. Scaling properties

As a systematic test of the scaling properties, non-unitary CCS propagation, by Eq. (73) was performed for the benchmark multidimensional Henon–Heiles systems, modelled by the Hamiltonian

$$H = \frac{1}{2}\sum_{m=1,M}\left(p_m^2+q_m^2\right) + \lambda\sum_{m=1,M-1}\left(q_m^2 q_{m+1} - q_{m+1}^3/3\right), \qquad (92)$$

with $\lambda = 0.11803$, which had previously been used to test the scaling properties of HK propagation [21,67]. Our reported calculations [34] included both the autocorrelation functions $\langle\Psi(0)|\Psi(t)\rangle$ and the spectra derived from their Fourier transforms for the 2D, 6D, 10D, and 14D models. Test 2D calculations, with single sum propagation by Eq. (73) showed excellent agreement with exact split-operator propagation, using 2000 trajectories generated either by a Sobol quasi-random 4D sequence algorithm [58] or by importance sampling. Split operator propagation is no longer feasible for higher dimensional models, but good agreement was obtained with HK spectral peak positions reported for 6D and 10D by Brewer [67]. However, loss of norm in the non-unitary CCS propagation leads to somewhat broader peaks. The same effect is seen in Fig. 5, which compares the CCS spectra for the 6D and 10D models, with those recently obtained by the multiconfiguration Hartree (MCH) method [68]. Again the peak positions are in good agreement, but the CCS peak widths are too broad. Note that an error in our previous 10D spectrum [34] has been removed by increasing the cut-off energy for acceptable trajectories from $E_{\mathrm{cut\,off}} = 15$ to

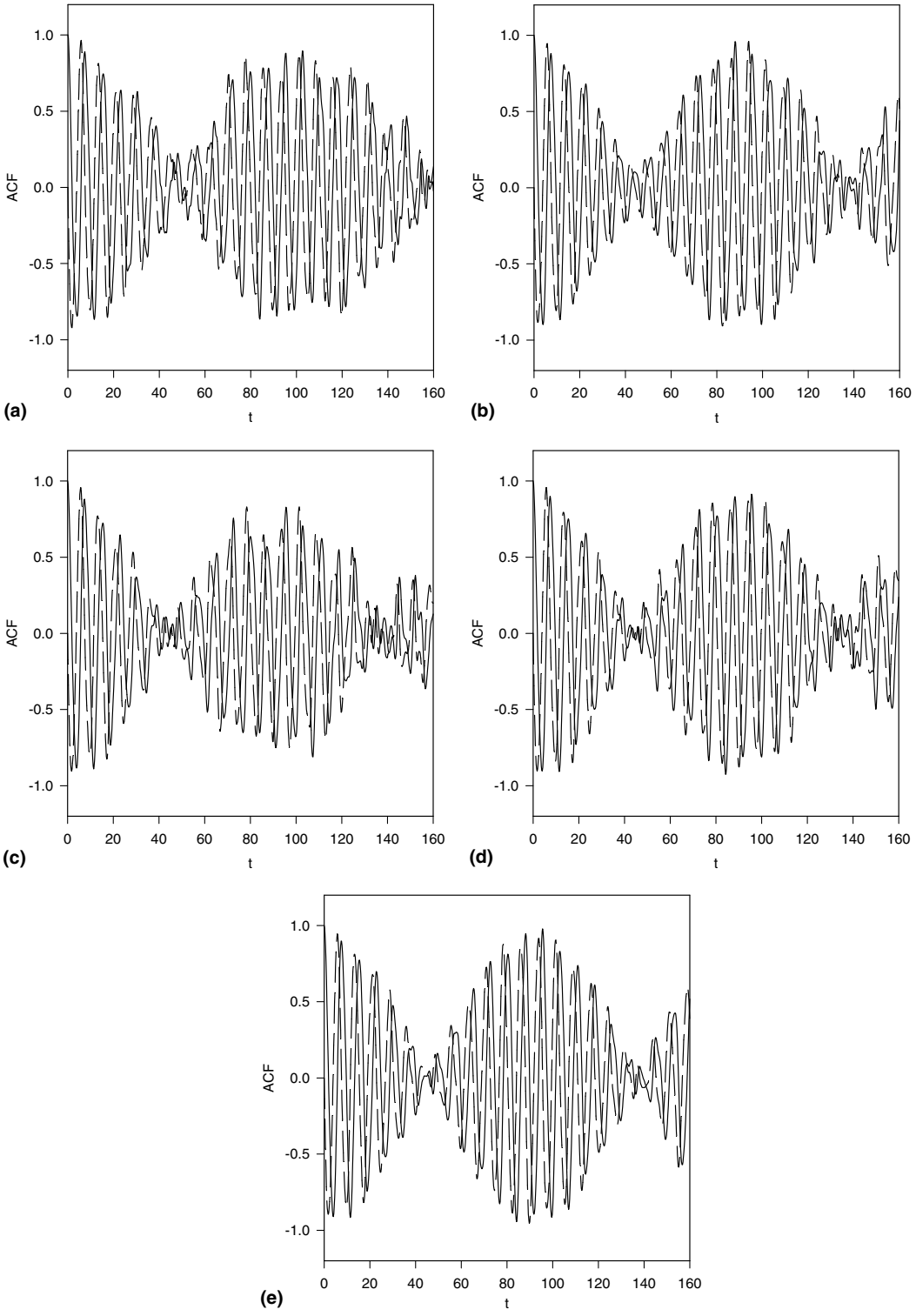

Fig. 4. Real (solid line) and imaginary (dashed line) part of ACF for our propagation on moving Monte Carlo grid for 200 (a) and 2000 (b) trajectories. The results for Sobol quasirandom grid are shown for 200 (c) and 500 (d) trajectories. For comparison the ACF obtained by "exact" split operator propagation is also shown (e). Reproduced from [33] with permission.

$E_{\text{cut off}} = 30$, because the previous cut-off seriously distorted the shape of the initial wavepacket.

With importance sampling, the CCS propagation was converged for the 2D, 6D and 10D models with 2000, 5000, and 10,000 trajectories, respectively, compared with 2000, 16,000 and 64,000 HK trajectories [67]. Seemingly the number of required trajectories scales roughly linearly with dimensionality for the CCS

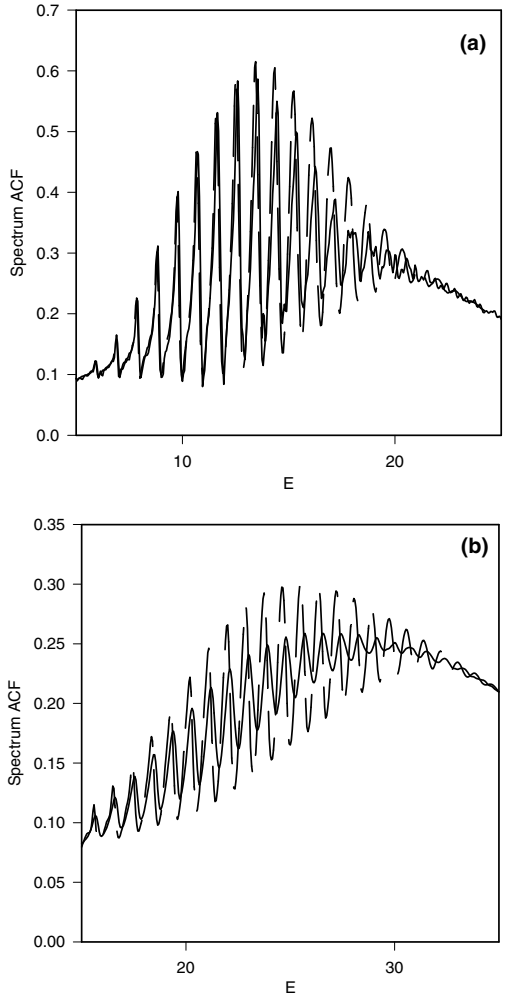

Fig. 5. The spectrum of the autocorrelation function for 6D (frame a) and 10D (frame b) problems obtained with the help of importance sampling compared with that obtained in [68] with the help of multi-configurational Hartree method.

method, compared with roughly quadratically for the HK method. However, it must be remembered that the quality of our 10D results worse then that of 6D. Nevertheless, in both HK and CCS techniques the scaling is markedly better than exponential.

More rigorous tests of the scaling properties was provided for uniform, rather than biased, Monte Carlo sampling. Propagation on a uniform grid can only be performed at much lower mean energies than those reported above, in order to avoid rapid dissociation of a large fraction of the sample. The procedure adopted is to choose a cut-off energy, $E_{\max}$, above the energies of a specified number (several hundred) of quantum states, N_{QS}, given by

$$N_{\mathrm{QS}} = \frac{\Gamma}{(2\pi\hbar)^M} = \int_{E<E_{\max}} \frac{\mathrm{d}^2\mathbf{z}}{\pi^M}. \tag{93}$$

Then we obtain the result with a given quality of norm conservation by the CCS method with N_{CS} basis CS, and use the ratio $k = N_{\mathrm{CS}}/N_{\mathrm{QS}}$ as a measure of the scaling with dimensionality. The resulting values of k for 2D, 6D and 10D were found to be roughly 10, 50 and 150, respectively, which is close to the quadratic scaling, $k \propto M^2$, expected for Monte Carlo integration. Notice that our random grid covers the phase space rather densely with many more then one CS in the volume occupied by a single quantum state. However, the CCS method still scales much better with dimensionality than calculation on a regular grid which would lead to exponential scaling $k = l^M$ and would result in $k \approx 10^3$ or 10^5 CS for 6D and 10D problems, respectively.

8.3. Stability and norm conservation

CCS calculations for Fermi resonance coupling in $v = 6$ CH stretching overtone manifold of CHD_3 [36], provide information on the relative computational efficiencies of the non-unitary single sum, Eq. (73), and unitary double sum, Eq. (81), for propagation times sufficient to obtain 10–20 cm^{-1} resolution at a total an energy of about 16,000 cm^{-1}. The model Hamiltonian [69,70] includes strong Fermi resonance coupling between the CH stretching mode, v_1 and the doubly degenerate bend, v_5, with weaker coupling to the other six vibrational modes.

As an initial test, results for the single sum and double sum propagations were compared with those obtained by split operator (SO) propagation [59,60] for a reduced 3D model involving only the Fermi coupled modes, v_1, v_{5a} and v_{5b}. We observed propagation remaining accurate only for a finite period of time, after which autocorrelation function decayed due to Monte Carlo error or to put it differently due to noise. For both unitary and non-unitary propagation decay time increases with the increase of the number of the CS. Stable propagation for up to 1 ps was achieved by the unitary and non-unitary schemes with 1000 and 5000 trajectories, respectively, in both cases the autocorrelation function showed weaker recurrences than for the split operator propagation, the attenuation of a strong recurrence peak at 0.7 ps being by a factor of about three in the unitary and five in the non-unitary case. The Fermi resonance splittings of about 100 cm^{-1} in the reported spectra [36], shown in Fig. 5, agree with the split operator splittings, with small uniform shifts of -20 cm^{-1} and $+40$ cm^{-1} in Fig. 5(a) and (b), respectively, compared with the split operator spectrum (not shown). The attenuation of the CCS autocorrelation functions also leads to broader lines than for the SO spectrum.

The two CCS approaches were also extended to the full nine vibrational mode problem, which becomes intractable for split-operator propagation, because the size of the required rectangular grid scales exponentially

with the number of degrees of freedom. Unitary and non-unitary propagation for up to 1 ps now required 2000 or 20,000 trajectories, in the two cases, with even more rapid attenuation than in the 3D case. The peak widths in the derived spectra in Fig. 5(c) and (d) are therefore broader than for the 3D model. Interaction with the bath modes appears to cause a shift in the overall spectrum of $\sim$140 cm^{-1} and an increase in the Fermi-resonance splitting by $\sim$20 cm^{-1}.

The first conclusion from this section is that spectra of comparable quality may be obtained by the unitary and non-unitary propagation schemes, using Eqs. (81) and (73), respectively, provided the number of trajectories is increased by a factor of 5–10 in the latter case. The main requirement is that the attenuation due to Monte Carlo inaccuracies is sufficiently well controlled to allow stable propagation for times of the order of 1 ps, corresponding to 100 cycles of the CH stretching mode. The unitary approach requires fewer trajectories, by a factor 5–10, and suffers less severely from attenuation; but the computational effort is actually greater than for the non-unitary propagation, due to the fact that the inverse overlap matrix Ω^{-1} enters into unitary equations at each step. This also eventually limits the number of trajectories that can be employed, due to the near singular character of Ω as the trajectory density increases. The second conclusion relates to the scaling with dimensionality, bearing in mind that the spectra in Fig. 6(a) and (b), for the 3D model are of higher quality than those in Fig. 6(c) and (d) for 9D. As a general rule, spectra of comparable quality may be obtained by increasing the number of trajectories by a factor of 10 in

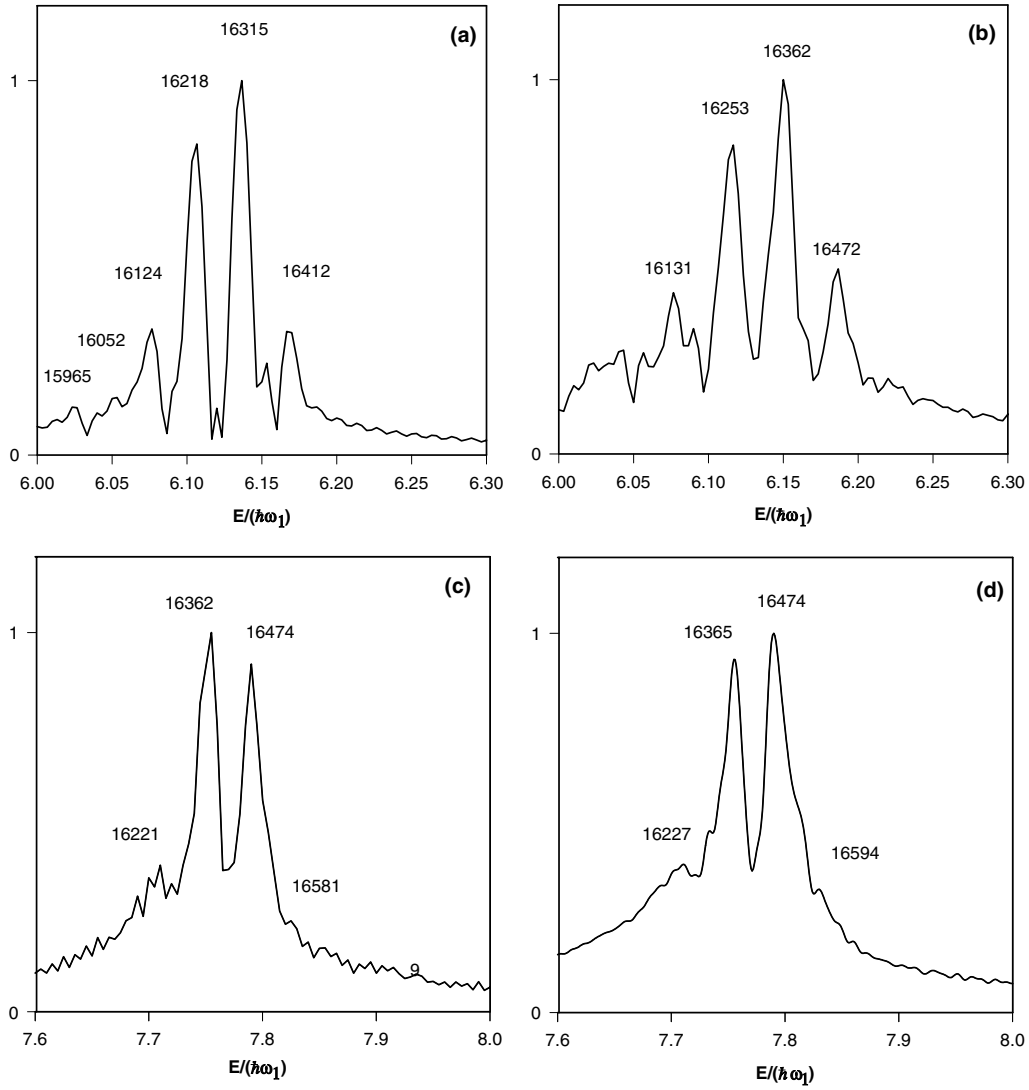

Fig. 6. Spectrum of the autocorrelation function obtained by the CCS method for CHD_3 model Hamiltonian. 3D problem unitary form (frame a). 3D problem non-unitary form (frame b). 9D problem unitary form (frame c). 9D problem non-unitary form (frame d). Reproduced from [36] with permission.

going from 3D to 9D, which is consistent with quadratic scaling.

9. Conclusions

The purpose of this review is to set the theory of phase space quantum initial value techniques, based on coherent states, in the context of an exact integro-differential form for the time-dependent Scrodinger equation. The use of a trajectory guided coherent state basis is shown to have enormous benefits in smoothing and reducing the magnitude of the integro-differential kernel, thereby exploiting the advantage of Monte Carlo sampling in controlling the growth of the computational effort with system size. The special properties of coherent states are also shown to allow the evaluation of Hamiltonian matrix elements 'on the fly'. Three discrete approximations were suggested, for use in practical application of this coupled coherent states (CCS) technique – a single sum non-unitary method, based on Eq. (73) and two double sum unitary schemes given by Eqs. (81) and (85).

In considering connections with other coherent state based theories, it should first be noted that the present systematic formulation requires that the underlying classical trajectories are determined by an averaged classical counterpart of the ordered Hamiltonian $\widehat{H}_{\mathrm{ord}}(\hat{a}^{\dagger},\hat{a})$, in which powers of $\hat{a}^{\dagger}$ and $\hat{a}$ are grouped to the right and left, respectively – a reordering that leads to an increase in minima and a decrease in the maxima of the classical potential function. By contrast, the semiclassical IVR methods of Heller [8] and Herman and Kluk (HK) [3,9,10,12,37] and the coupled quantum mechanical approaches of Metiu and co-workers [23,24], Martinez et al. [25–29] and Burghardt et al. [30,31] all employ trajectories determined by the simple classical Hamiltonian. It was shown in Section 6 that Heller's method corresponds to complete neglect of the quantum mechanical coupling between different trajectories, while analytical solution of the CCS equations within a local quadratic approximation yields either the Herman–Kluk prefactor, by a method due to Miller [38], or the coherent state matrix of the Herman–Kluk propagator, by a method due to the present authors [35]. The simplified exposition given in Section 6 starts by employing a quadratic approximation around a trajectory determined by the classical Hamiltonian, in which case the HK results are recovered exactly, whereas more detailed analysis involving a locally quadratic expansion around a trajectory of the averaged Hamiltonian, $H_{\mathrm{ord}}(z^{*},z)$ yields an additional phase correction.

Turning to computational aspects, the effort involved by all the methods cited have much more favorable scaling properties with system size, than the exponential scaling expected for multimensional regular grid techniques. The single trajectory, Heller and HK, approaches have the advantage that the effort is simply proportional to the number of trajectories employed. In addition the scaling test performed by Brewer [67] shows that the number of HK trajectories required for convergence scales roughly quadratically with the dimensionality of the problem. Also steps have been taken to reduce the number of trajectories needed to converge the semiclassical IVR by means of smoothening in space [20,21] or time [71]. The CCS method is designed to handle purely quantum mechanical effects such as tunneling, which cannot be treated directly by the single trajectory approaches. The computational cost now scales quadratically with the number of trajectories and Monte Carlo sampling leads to the quadratic scaling with dimensionality in the number of trajectories. Finally, it is interesting to compare the convergence properties of the non-unitary, single sum and unitary double sum CCS propagation methods given by Eqs. (73) and (81), respectively. Bearing in mind that in practice one solves a system of linear equations, rather than computing the inverse matrix Ω^{-1}, the computational effort in both cases scales quadratically with the number of trajectories,. The proportionality factor is greater for the double sum methods, but the convergence with respect to the number of trajectories is found to be faster. The overall effort is therefore comparable by both unitary and non-unitary methods.

In summary, the CCS method is a new computational tool, firmly based in quantum mechanics and with excellent scaling properties with the dimensionality of the system. The method of derivation also provides a framework against which to assess a variety of other phase space based computational methods.

Acknowledgements

One of the authors (D.V.S.) gratefully acknowledges financial support from the UK EPSRC.

Appendix A

All formulas in this section have been given for 1D case. The generalization for M-dimensions is trivial. The integration must be done over the whole multidimensional phase space, so that the identity operator becomes

$$\widehat{I}=\frac{1}{\pi^{M}}\int \mathrm{d}^{2}\mathbf{z}|\mathbf{z}\rangle\langle\mathbf{z}|, \tag{A.1}$$

where $\mathrm{d}^{2}\mathbf{z}=\prod_{i=1,M}\frac{\mathrm{d}q_i\,\mathrm{d}p_i}{2\hbar}$ and all variables are replaced by corresponding vectors. For example, Eq. (3) becomes

$$\langle \mathbf{x}|\mathbf{z}\rangle = \left(\frac{\gamma}{\pi}\right)^{\frac{M}{4}} \exp\left(-(\mathbf{x}-\mathbf{q})^{\top}\frac{\gamma}{2}(\mathbf{x}-\mathbf{q}) + \frac{\mathrm{i}}{\hbar}\mathbf{p}(\mathbf{x}-\mathbf{q}) + \frac{\mathbf{ipq}}{2\hbar}\right). \tag{A.2}$$

Eqs. (13), (9), (10) and (19) read as

$$\langle \mathbf{z}_2|\mathbf{z}_1\rangle = \exp\left(\mathbf{z}_2^{*}\mathbf{z}_1 - \frac{|\mathbf{z}_2|^2}{2} - \frac{|\mathbf{z}_1|^2}{2}\right), \tag{A.3}$$

$$\left\langle \mathbf{z}_2\middle|\widehat{H}\middle|\mathbf{z}_1\right\rangle = \langle \mathbf{z}_2|\mathbf{z}_1\rangle H_{\mathrm{ord}}\left(\mathbf{z}_2^{*},\mathbf{z}_1\right), \tag{A.4}$$

$$\frac{\mathrm{d}\mathbf{z}}{\mathrm{d}t} = -\frac{\mathrm{i}}{\hbar}\frac{\partial H_{\mathrm{ord}}(\mathbf{z}^{*},\mathbf{z})}{\partial \mathbf{z}^{*}}, \quad \frac{\mathrm{d}\mathbf{z}^{*}}{\mathrm{d}t} = \frac{\mathrm{i}}{\hbar}\frac{\partial H_{\mathrm{ord}}(\mathbf{z}^{*},\mathbf{z})}{\partial \mathbf{z}}, \tag{A.5}$$

$$S_z = \int\left[\frac{\mathrm{i}\hbar}{2}\left(\mathbf{z}^{*}\frac{\mathrm{d}\mathbf{z}}{\mathrm{d}t} - \frac{\mathrm{d}\mathbf{z}^{*}}{\mathrm{d}t}\mathbf{z}\right) - H_{\mathrm{ord}}(\mathbf{z}^{*},\mathbf{z})\right]\mathrm{d}t, \tag{A.6}$$

correspondently, where all products are scalar products of M-dimensional vectors. The integro-differential Eqs. (25) and (37) generalise to

$$\frac{\mathrm{d}\langle \mathbf{z}|\Psi\rangle}{\mathrm{d}t} = -\frac{\mathrm{i}}{\hbar}\int\left\langle \mathbf{z}\middle|\widehat{H}\middle|\mathbf{z}'\right\rangle\langle \mathbf{z}'|\Psi\rangle\frac{\mathrm{d}^2\mathbf{z}'}{\pi^M} \tag{A.7}$$

and

$$\frac{\mathrm{d}C(\mathbf{z}(t))}{\mathrm{d}t} = -\frac{\mathrm{i}}{\hbar}\int\langle \mathbf{z}|\mathbf{z}'\rangle\,\delta^2 H_{\mathrm{ord}}\left(\mathbf{z}^{*},\mathbf{z}'\right)C\left(\mathbf{z}'(t)\right) \times \exp\left(\frac{\mathrm{i}}{\hbar}(S_{z'}-S_z)\right)\frac{\mathrm{d}^2\mathbf{z}'}{\pi^M}, \tag{A.8}$$

where

$$\delta^2 H_{\mathrm{ord}}\left(\mathbf{z}^{*},\mathbf{z}'\right) = H_{\mathrm{ord}}\left(\mathbf{z}^{*},\mathbf{z}'\right) - H_{\mathrm{ord}}(\mathbf{z}^{*},\mathbf{z}) - \frac{\partial H_{\mathrm{ord}}(\mathbf{z}^{*},\mathbf{z})}{\partial \mathbf{z}}\left(\mathbf{z}'-\mathbf{z}\right) \approx \frac{1}{2}\left(\mathbf{z}'-\mathbf{z}\right)^{\top}\frac{\partial^2 H_{\mathrm{ord}}}{\partial \mathbf{z}^2}\left(\mathbf{z}'-\mathbf{z}\right)+\cdots. \tag{A.9}$$

Finally, in the Herman–Kluk propagator formula (68)

$$|\Psi\rangle = \int|\mathbf{z}(t)\rangle\sqrt{\det\mathbf{M}_{zz}}\exp\left(\frac{\mathrm{i}S_z^{\mathrm{cl}}}{\hbar}\right)\langle \mathbf{z}(0)|\Psi(0)\rangle\frac{\mathrm{d}^2\mathbf{z}}{\pi^M}, \tag{A.10}$$

the determinant of $\mathbf{M}_{zz}$ block of the monodromy matrix should be used.

Appendix B

The estimation of integrals in Eqs. (61) and (62) is tedious but fairly straightforward. Let us look first at the product $\langle z(t)|z'(t)\rangle\exp\left(\frac{\mathrm{i}}{\hbar}(S_{z'}-S_z)\right)\langle z'(0)|z_i(0)\rangle$, which enters into both integrals I_2 and I_0. Here z_i is the center of the propagating wave packet, z is the reference CS under consideration and $z' = z+\Delta z$ is a CS in the vicinity of z. By using Eq. (13) it is easy to see that

$$\left\langle z'(0)|z_i(0)\right\rangle = \left\langle z'(0)|z(0)\right\rangle\langle z(0)|z_i(0)\rangle \times \exp\left[\Delta z^{*}(0)(z_i(0)-z(0))\right]. \tag{B.1}$$

The factor $\langle z(0)|z_i(0)\rangle$ is the same for both I_2 and I_0 and cancels out of their ratio. Also

$$\left\langle z'(0)|z(0)\right\rangle = \exp\left[\frac{\mathrm{i}}{2}(\Delta z^{*}(0)z(0) - \Delta z(0)z^{*}(0)) - \frac{|\Delta z(0)|^2}{2}\right], \tag{B.2}$$

and similarly for $\langle z(t)|z'(t)\rangle$

$$\left\langle z(t)|z'(t)\right\rangle = \exp\left[-\frac{\mathrm{i}}{2}(\Delta z^{*}(t)z(t) - \Delta z(t)z^{*}(t)) - \frac{|\Delta z(t)|^2}{2}\right]. \tag{B.3}$$

The ratio of two integrals can now be written as

$$\frac{I_2}{I_0} = \left\{\int\exp\left[-\frac{|\Delta z(t)|^2}{2}-\frac{|\Delta z(0)|^2}{2}\right] \times\exp\left[\Delta z^{*}(0)(z_i(0)-z(0))\right]\exp[\Phi](\Delta z^{*}(t))^2\frac{\mathrm{d}^2 z'}{\pi}\right\}\Bigg/ \left\{\int\exp\left[-\frac{|\Delta z(t)|^2}{2}-\frac{|\Delta z(0)|^2}{2}\right]\exp[\Phi]\frac{\mathrm{d}^2 z'}{\pi}\right\}, \tag{B.4}$$

where

$$\Phi = \mathrm{i}\left[-\frac{(\Delta z^{*}(t)z(t)-\Delta z(t)z^{*}(t))}{2}+\frac{\Delta S}{\hbar} + \frac{(\Delta z^{*}(0)z(0)-\Delta z(0)z^{*}(0))}{2}\right]. \tag{B.5}$$

Initially at $t=0$

$$\Phi = 0, \tag{B.6}$$

and it is easy to show that in local quadratic approximation

$$\frac{\mathrm{d}\Phi}{\mathrm{d}t} = 0, \tag{B.7}$$

such as Eq. (B.6) holds for all times. Indeed, local quadratic approximation means that the Hamiltonian has a form

$$H = \frac{p^2}{2m} + aq^2 + bq + c. \tag{B.8}$$

From the action Eq. (19) it is easy to see that $\mathrm{d}S/\mathrm{d}t = -bq/2$ and therefore

$$\frac{\mathrm{d}\Delta S}{\mathrm{d}t} = -\frac{b\Delta q}{2}. \tag{B.9}$$

From Hamilton's equations it follows that

$$\frac{\mathrm{d}}{\mathrm{d}t}\left[-\frac{(\Delta z^* z - \Delta z z^*)}{2}\right] = \frac{\mathrm{d}}{\mathrm{d}t}\left[\frac{(\Delta q p - \Delta p q)}{2}\right] = \frac{b\Delta q}{2}, \tag{B.10}$$

such that Eqs. (B.9) and (B.10) prove Eq. (B.7) and the factor $\exp[\Phi]$ can be removed from Eq. (B.4). Now to perform the integration one has to replace z by q and p and notice that initial $\Delta q(0)$, $\Delta p(0)$ and final Δq, Δp are related through Eq. (58). After that the integrals I_2 and I_0 become simple Gaussian and their ratio can be evaluated yielding

$$\frac{I_2}{I_0} = 2\frac{\left(M_{qq} - M_{pp} - i\gamma\hbar M_{qp} - \frac{\mathrm{i}}{\gamma\hbar}M_{pq}\right)}{\left(M_{qq} + M_{pp} - i\gamma\hbar M_{qp} + \frac{\mathrm{i}}{\gamma\hbar}M_{pq}\right)} = -2\frac{M_{z^*z}}{M_{zz}}. \tag{B.11}$$

References

[1] W.H. Miller, T.F. George, J. Chem. Phys. 56 (1972) 5668.
[2] M.S. Child, Semiclassical Methods with Molecular Applications, Clarendon Press, Oxford, 1991.
[3] M.F. Herman, Annu. Rev. Phys. Chem. 45 (1994) 83.
[4] M.A. Sepulveda, F. Grossmann, in: I. Prigogine, S.A. Rice (Eds.), Advances in Chemical Physics, vol. XCVI, Wiley, New York, 1999, p. 191.
[5] F. Grossmann, Comments Atom. Mol. Phys. 34 (1999) 141.
[6] D.J. Tannor, S. Garashchuk, Annu. Rev. Phys. Chem. 51 (2000) 553.
[7] W.H. Miller, J. Phys. Chem. A105 (2001) 2942.
[8] E.J. Heller, J. Chem. Phys. 75 (1981) 2923.
[9] M.F. Herman, E. Kluk, Chem. Phys. 91 (1984) 27.
[10] E. Kluk, M.F. Herman, H.L. Davis, J. Chem. Phys. 84 (1986) 326.
[11] J.H. Van Vleck, Proc. Natl. Acad. Sci. USA 14 (1928) 178.
[12] K. Kay, J. Chem. Phys. 100 (1994) 4377;
K. Kay, J. Chem. Phys. 100 (1994) 4432;
K. Kay, J. Chem. Phys. 101 (1994) 2250.
[13] M. Toss, W.H. Miller, G. Stock, J. Chem. Phys. 112 (2000) 10282.
[14] V. Guallar, V.S. Batista, W.H. Miller, J. Chem. Phys. 110 (1999) 9922;
V. Guallar, V.S. Batista, W.H. Miller, J. Chem. Phys. 113 (2000) 9510.
[15] X. Sun, W.H. Miller, J. Chem. Phys. 106 (1997) 916.
[16] S. Bonella, D.F. Coker, Chem. Phys. 268 (2001) 189;
J. Chem. Phys. 114 (2001) 7778.
[17] G. Campolieti, P. Brumer, J. Chem. Phys. 107 (1997) 791;
G. Campolieti, P. Brumer, J. Chem. Phys. 109 (1998) 2999.
[18] V.S. Batista, P. Brumer, J. Phys. Chem. A 105 (2001) 2591.
[19] V.S. Batista, P. Brumer, J. Chem. Phys. 114 (2001) 10321.
[20] A.R. Walton, D.E. Manolopoulos, Mol. Phys. 87 (1996) 961.
[21] H. Wang, D.E. Manolopoulos, W.H. Miller, J. Chem. Phys. 115 (2001) 6317.
[22] M. Ovchinnikov, V.A. Apkarian, J. Chem. Phys. 108 (1998) 2277.
[23] S.I. Sawada, R. Heather, B. Jackson, H. Metiu, J. Chem. Phys. 83 (1985) 3009.
[24] S.I. Sawada, H. Metiu, J. Chem. Phys. 84 (1986) 227.
[25] T. Martinez, R.D. Levine, Chem. Phys. Lett. 259 (1996) 252;
J. Chem. Phys. 105 (1996) 6334.
[26] M. Ben-Nun, T. Martinez, J. Chem. Phys. 104 (2000) 5161;
M. Ben-Nun, T. Martinez, J. Chem. Phys. 108 (1998) 7244;
M. Ben-Nun, T. Martinez, J. Chem. Phys. 110 (1999) 4134;
M. Ben-Nun, T. Martinez, J. Chem. Phys. 112 (2003) 6113.
[27] T. Martinez, M. Ben-Nun, R.D. Levine, J. Phys. Chem. 100 (1996) 7884.
[28] T. Martinez, M. Ben-Nun, J. Chem. Soc. Faraday Trans. 93 (1997) 940.
[29] M. Ben-Nun, T.J. Martinez, in: I. Prigogine, S.A. Rice (Eds.), Advances in Chemical Physics, vol. 121, Wiley, New York, 2002, p. 439.
[30] I. Burghardt, H.-D. Meyer, L.S. Cederbaum, J. Chem. Phys. 111 (1999) 2927.
[31] G.A. Worth, I. Burghardt, Chem. Phys. Lett. 368 (2003) 502.
[32] D.V. Shalashilin, M.S. Child, J. Chem. Phys. 113 (2000) 10028.
[33] D.V. Shalashilin, M.S. Child, J. Chem. Phys. 114 (2001) 9296.
[34] D.V. Shalashilin, M.S. Child, J. Chem. Phys. 115 (2001) 5367.
[35] M.S. Child, D.V. Shalashilin, J. Chem. Phys. 118 (2003) 2061.
[36] D.V. Shalashilin, M.S. Child, J. Chem. Phys. 119 (2003) 1961.
[37] W.H. Miller, Mol. Phys. 100 (2002) 397.
[38] W.H. Miller, J. Phys. Chem. 106 (2002) 8132.
[39] J.B. Anderson, in: S.R. Langhoff (Ed.), Quantum Mechanical Electronic Structure Calculations with Chemical Accuracy, Kluwer, Dordrecht, 1995.
[40] J.R. Klauder, B.-S. Skagerstam, Coherent States, World Scientific, Singapore, 1985.
[41] W.H. Louisell, Quantum Statistical Properties of Radiation, Wiley, New York, 1973.
[42] A. Perelomov, Generalized Coherent States and Their Applications, Springer, New York, 1986.
[43] D.V. Shalashilin, B. Jackson, Chem. Phys. Lett. 318 (2000) 305.
[44] J.C. Burant, V. Batista, J. Chem. Phys. 116 (2002) 2748.
[45] J. von Neumann, Mathematical Foundations of Quantum Mechanics, Princeton Universty Press, Princeton, 1985.
[46] D. Huber, E.J. Heller, J. Chem. Phys. 87 (1987) 5302.
[47] D. Huber, E.J. Heller, J. Chem. Phys. 89 (1988) 4752.
[48] D. Huber, Song Ling, D.G. Imre, E.J. Heller, J. Chem. Phys. 90 (1989) 7317.
[49] L.M. Andersson, J. Chem. Phys. 115 (2001) 1158.
[50] M. Thoss, G. Stock, Phys. Rev. A 59 (1999) 65.
[51] E.J. Heller, J. Chem. Phys. 62 (1975) 1544.
[52] M. Baranger, M.A.M. de Aguiar, F. Keck, H.J. Kosch, B. Schellhaaß, J. Phys. A 34 (2001) 7227.
[53] F. Grossman, M.F. Herman, J. Phys. A 34 (2002) 9489.
[54] M. Baranger, M.A.M. de Aguiar, F. Keck, H.J. Kosch, B. Schellhaaß, J. Phys. A 35 (2002) 9793.
[55] M. Baranger, M.A.M. de Aguiar, H.J. Kosch, J. Phys. A 35 (2002) 9795.
[56] M.S. Child, Y. Sturdy, P. Sherrat, J. Phys. Chem., submitted.
[57] C. Harabati, J.M. Rost, F. Grossman, J. Chem. Phys. 120 (2004) 26.
[58] W.H. Press, B.P. Flannery, S.A. Teukolsky, W.T. Vetterling, Numerical Recipes: The Art of Scientific Computing, second ed., Cambridge Univesity Press, Cambridge, 1992.
[59] R. Kosloff, J. Phys. Chem. 92 (1988) 2087.
[60] M.D. Feit, J.A. Fleck, J. Chem. Phys. 78 (1983) 301;
M.D. Feit, J.A. Fleck, J. Chem. Phys. 80 (1984) 2578.
[61] C. Leforestier, R. Bisseling, C. Cerjan, M.D. Feit, R. Friesner, A. Hammerich, G. Jolicard, W. Karrlein, H.D. Meyer, N. Lipkin, O. Roncero, R. Kosloff, J. Comput. Phys. 94 (1991) 59.
[62] V.A. Mandelshtam, M. Ovchinnikov, J. Chem. Phys. 108 (1998) 9206.
[63] V.A. Mandelshtam, H.S. Taylor, J. Chem. Phys. 107 (1997) 6756;
V.A. Mandelshtam, H.S. Taylor, J. Chem. Phys. 108 (1998) 9970.

[64] V.A. Mandelshtam, J. Chem. Phys. 108 (1998) 9999.
[65] M. Ovchinnikov, private communication.
[66] V.A. Benderskii, D.E. Makarov, P.G. Grinevich, Chem. Phys. 170 (1993) 275.
[67] M.L. Brewer, J. Chem. Phys. 111 (1999) 6168.
[68] M. Nest, H.-D. Meyer, J. Chem. Phys. 117 (2002) 10499.
[69] C. Iung, C. Leforestier, J. Chem. Phys. 90 (1989) 3198; C. Iung, C. Leforestier, J. Chem. Phys. 97 (1992) 2481.
[70] C. Iung, C. Leforestier, R.E. Wyatt, J. Chem. Phys. 98 (1993) 6722.
[71] A.L. Kaledin, W.H. Miller, J. Chem. Phys. 118 (2003) 7174; A.L. Kaledin, W.H. Miller, J. Chem. Phys. 119 (2003) 3078.